Spatio-Temporal Control of the Phase Separation of Chemically Active Immotile Colloids

Journal:	*National Science Open*
Manuscript ID	NSO20230050.R1
Manuscript Type:	Research Article
Date Submitted by the Author:	27-Sep-2023
Complete List of Authors:	Peng, Yixin; Harbin Institute of Technology Shenzhen Li, Longfei; Chinese Academy of Sciences Guo, Shutong; Shanghai Jiao Tong University Chen, Xi; Harbin Institute of Technology Shenzhen Zhou, Chao; Harbin Institute of Technology Shenzhen Xing, Dingyu; Harbin Institute of Technology Zhang, H. P.; Shanghai Jiao Tong University Yang, Mingcheng; Institute of Physics Chinese Academy of Sciences Wang, Wei; Harbin Institute of Technology Shenzhen,
Keywords:	phase separation, colloids, active matter, non-equilibrium, structured light, pattern formation
Note: The following files were submitted by the author for peer review, but cannot be converted to PDF. You must view these files (e.g. movies) online.	
Supplementary videos_1.rar	

RESEARCH ARTICLE

National Science Open

1: 2022xxxx, 2022

https://doi.org/10.1360/nso/xxxxxxxx

Physics

Special Topic: Physics on Active Matter

Spatio-Temporal Control of the Phase Separation of Chemically Active Immotile Colloids

Yixin Peng[1,#], Longfei Li[2,#], Shutong Guo[3], Xi Chen[1], Chao Zhou[1], Dingyu Xing[4], H. P. Zhang[3,*], Mingcheng Yang[2,5,*], Wei Wang[1,*]

[1]*School of Materials Science and Engineering, Harbin Institute of Technology (Shenzhen), Shenzhen, 518055, China;*

[2]*Beijing National Laboratory for Condensed Matter Physics and Laboratory of Soft Matter Physics, Institute of Physics, Chinese Academy of Sciences, Beijing 100190, China ;*

[3] *School of Physics and Astronomy, Institute of Natural Sciences and MOE-LSC, Shanghai Jiao Tong University, Shanghai 200240, China;*

[4]*School of Civil and Environmental Engineering, Harbin Institute of Technology (Shenzhen), Shenzhen, 518055, China*

[5]*School of Physical Sciences, University of Chinese Academy of Sciences, Beijing 100049, China*

#Contributed equally to this work.

*Corresponding authors (emails: weiwangsz@hit.edu.cn (Wei Wang); mcyang@iphy.ac.cn (Mingcheng Yang); hepengzhang@sjtu.edu.cn (H. P. Zhang)

Received 13 August 2023; Revised 27 September 2023; Accepted 20 October 2023; Published online

Abstract:

Understanding and controlling phase separation in nonequilibrium colloidal systems is of both fundamental and applied importance. In this article, we investigate the spatiotemporal control of phase separation in chemically active immotile colloids. We show that a population of silver colloids can spontaneously phase separate into dense clusters in hydrogen peroxide (H_2O_2) due to phoretic attraction. The characteristic length of the formed pattern was quantified and monitored over time, revealing a growth and coarsening phase with different growth kinetics. By tuning the trigger frequency of light, the lengths and growth kinetics of the clusters formed by silver colloids in H_2O_2 can be controlled. In addition, structured light was used to precisely control the shape, size, and contour of the phase-separated patterns. This study provides insight into the microscopic details of the phase separation of chemically active colloids induced by phoretic attraction, and presents a generic strategy for controlling the spatiotemporal evolution of the resulting mesoscopic patterns.

Keywords: phase separation, colloids, active matter, non-equilibrium, structured light, pattern formation

INTRODUCTION

Mixtures can phase separate in systems driven away from thermal equilibrium by external energy input. Such non-equilibrium phase separation is widely found from colloids [1-3] and polymers [4, 5], to biological processes [6, 7] and astrophysical events [8]. Understanding non-equilibrium phase separation enables the development of materials with tailored electrical, magnetic and optical properties, while advancing research fields such as soft matter physics, materials science, chemistry and biology. A grand challenge of non-equilibrium phase separation lies in its spatiotemporal control, which involves manipulating the formation, growth, and organization of structures in non-equilibrium systems in real-time.

Colloids are an excellent model system for addressing this problem, as they are highly tunable in particle sizes, shapes, and interactions. Examples of non-equilibrium phase separation in colloids include self-propelled Janus particles exhibiting motility-induced phase separation [9-12], charged colloids that develop into tunable colloid crystal and colloidal swarms under external electric fields [13], and three dimensional structures of DNA-functionalized colloids responding to environmental changes [14]. Among them, phase separation mediated by chemically induced interaction is particularly attractive because of the long range nature of interparticle interactions, the ease of experimental setup, and the large library of chemical reactions to choose from. Notable examples include dynamic, motile clusters formed by Fe_2O_3 [15] or AuPt colloids [16, 17] that phoretically attract each other, and bio-mimicking, shape-morphing clusters formed by chemically interacting colloids [2, 18].

Despite these demonstrations of non-equilibrium phase separation in chemically active colloids, there has been limited control over the resulting patterns, including their shapes, sizes, and evolution kinetics. In this study, we address this gap by using the phase separation of *chemically active but immotile* silver (Ag)-coated microspheres as a model system. We have previously reported that such microspheres form clusters of growing sizes in H_2O_2 [19], similar to those formed by Au microspheres in N_2H_4 aqueous solutions [20], and clusters formed by by TiO_2 [21] or AgCl microparticles under UV light [22]. Here, we clarify the microscopic details of the phase separation of Ag colloids, quantify the characteristic length of the mesoscopic patterns and monitor their evolution kinetics, and develop a technique based on structured light to control such phase separation in both space and time. These findings deepen our understanding of the fundamental principles governing non-equilibrium phase separation, and could inspire new avenues for the controlled assembly of colloidal matter in applications of colloidal lasers [23], swarm control of microrobots [24], and encryption [25].

RESULTS AND DISCUSSIONS

Phase separation of Ag colloids: phenomenon and kinetics. Our following discussion is based on the key observation that silicon dioxide (SiO_2) microspheres half-coated with silver (Ag) (Fig. 1a) attracted each other in H_2O_2 (Fig. 1b) and formed clusters. These clusters were loose, long and interconnected at the beginning, but over time grew larger, more round in shape and more separte from each other. Two phases were formed, one is the cluster that liquid-like, and the other is the gas-like voids between clusters where colloids sparsely populated. An example is given in Fig. 1c and Video S1, where 5 μm SiO_2-Ag microspheres of a population density of 17% suspended in 0.001 w.t.% H_2O_2 formed clusters of ~100 μm in size in 100-200 s.

Janus SiO_2-Ag microspheres (referred to hereafter as "Ag colloids") were used throughout this study because they were more uniform in size, less likely to stick to each other or to the substrate, and formed clusters of more regular shapes than pure Ag microspheres, which showed qualitatively the same phase separation (Fig. S5 and Video S2). Also note that although Janus SiO_2-Ag microspheres are known to self-propel in H_2O_2 [26, 27], they become essentially immotile when the population density is larger than 4% (17% for the current study) due to the elevated ionic strength from the dissolution of Ag in H_2O_2 that suppresses the motility of Ag colloid, as explained in details in a previous study [19].

We describe the phase separation kinetics of Ag colloids by measuring the 2D packing fraction (Fig. 1d) and characteristic length (Fig. 1e) of the formed clusters as a function of time. The characteristic length is obtained by calculating the spatial correlation function (see Fig. S3 for details). Phase separation proceeded in two stages--growth and coarsening--that can be

distinguished by calculating the first derivative of the packing fraction over time (Fig. S6). In the growth stage (0-46 s in the example in Fig. 1), Ag particles quickly formed small clusters, which continued to attract surrounding particles until all particles entered the clusters. During this stage, the packing fraction of the clusters rapidly increased to its maxima, and the characteristic length grew with $\sim t^{0.22}$, where t is the elapsed time. Next, the population of Ag colloids transitioned to the coarsening stage (46-200 s), in which the clusters fused with each other. The packing fraction of the clusters during this stage decreased slightly over time, possibly because clusters grew denser and into 3D. The characteristic length during the coarsening stage first increased with $\sim t^{1.2}$ (46-96 s), then slowed down to $\sim t^{0.11}$ (96-200 s) due to the formation of large clusters that were too far apart to merge.

The power coefficient over time of only the growth stage is used below to describe the temporal evolution of the clusters of Ag colloids, not only because the coefficients in the coarsening stage are more complex, but also because the backbone structures of the phase separated patterns have already formed during the growth stage.

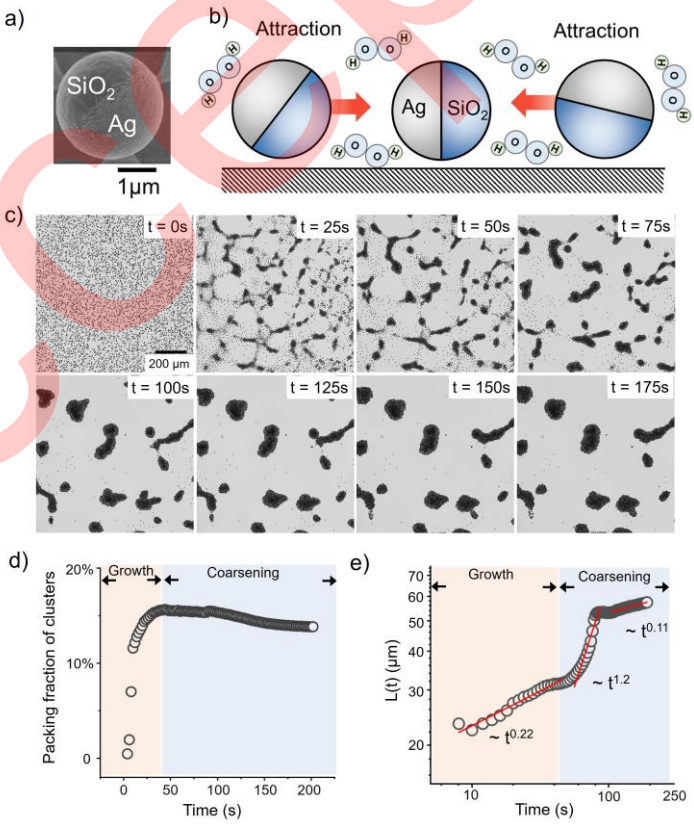

Figure 1 Phase separation of Ag colloids. a) Scanning electron micrograph of a SiO_2-Ag microsphere. b) SiO_2-Ag particles attract each other in dilute H_2O_2. c) Optical micrographs of the phase separation of SiO_2-Ag (dark) with population density φ=17% in 0.001 w.t.% H_2O_2 aqueous solution. d) The 2D

packing fraction of clusters and e) the characteristic length of the clusters in (c) as a function of time. The particle density is obtained by identifying the area fraction of the particles by imageJ, see Fig. S2 for details. The characteristic length (L) refers to the length corresponding to the first root of the spatial correlation function of the micrographs, see Fig. S3 for details. Both the x and y axis in (e) are in log10 scale. Solid red lines in (e) are linear fits.

Phase separation of Ag colloids: microscopic details. We propose that Ag colloids attract each other by ionic diffusiophoresis (Fig. 2a). To elaborate, we propose that Ag colloids are oxidized in H_2O_2 by:

$$Ag + 1/2\ H_2O_2 = Ag^+ + OH^- \qquad \text{Eqn. 1}$$

An Ag colloid thus releases Ag^+ and OH^-, the latter diffusing much faster than the former (5.27×10^{-9} m^2 s^{-1} vs 1.65×10^{-9} m^2 s^{-1}) [27, 28]. To maintain charge neutrality in the bulk solution, an electric field is generated that points from an Ag colloid outward. Nearby negatively charged colloidal particles thus migrate toward the ion-releasing colloid by electrophoresis (F_{EP}), a process known as ionic diffusiophoresis. At the same time, the same electric field pushes the positively charged layer of the fluid above the negatively charged bottom substrate. The resulting ionic diffusio-osmotic flow pushes the colloidal particles away from the ion-releasing Ag colloid (F_{EO}). Thus, F_{EP} and the F_{EO} have the same physical origin but point in opposite directions. According to the Smoluchowski equation [29], the drift velocity of the particle $\boldsymbol{u}$ is given as:

$$\boldsymbol{u} = -\frac{\varepsilon\,\zeta_p\,\boldsymbol{E}}{\eta} + \frac{\varepsilon\,\zeta_s\,\boldsymbol{E}}{\eta} = \frac{\varepsilon\,(\zeta_s - \zeta_p)\,\boldsymbol{E}}{\eta} \qquad \text{Eqn. 2}$$

Where ε is the permittivity of the solution, ζ_p and ζ_s are the surface zeta potentials of particle and substrate respectively, and $\boldsymbol{E}$ is the electric field. In our experiments, the zeta potential is -51.2 mV for pure Ag colloids, -56.9 mV for SiO_2 microspheres, and -44.6 mV for the glass substrate (see Supporting Information for measurement). Accordingly, we speculate that the net transport of a Janus SiO_2-Ag microsphere is dominated by electrophoresis ($F_{EP}>F_{EO}$), so that an Ag colloid attracts its neighbors and they collectively form a cluster.

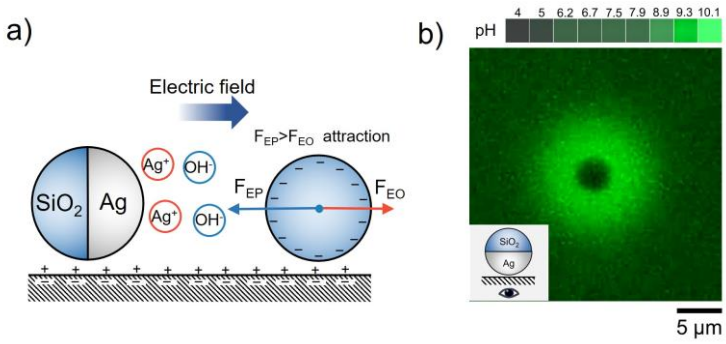

Figure 2 Ag colloids attract each other by ionic diffusiophoresis. a) Schematic diagram of a SiO_2-Ag microsphere attracting an inert microsphere by ionic diffusiophoresis in H_2O_2. The Ag cap reacts with H_2O_2 and releases Ag^+ and OH^-, which leads to a self-generated electric field that points away from the Ag colloid. A negatively charged tracer nearby reacts to this electric field by electrophoretically migrating toward the Ag colloid under the influence of an electrophoretic force F_{EP}. In addition, the electric field causes an electroosmotic flow from the negatively charged bottom substrate that advects the tracer via an electroosmotic draf force F_{EO}. F_{EP} dominates over F_{EO}, so that tracers are attracted to Ag colloids. b) Fluorescence photograph of SiO_2-Ag in 0.01 w.t.% H_2O_2. Stronger green fluorescence indicates higher pH values. A pH-sensitive fluorescent dye Solvent Green 7 was used at a concentration of 100 μM. Blue light of 475 nm and ~75 mW cm^{-2} was used to excite fluorescence.

This mechanism based on ionic diffusiophoresis is qualitatively supported by two pieces of evidence. First, using a pH-sensitive fluorescence probe molecule [24, 30], we detected a significant increase in pH near a Ag colloid in H_2O_2 (Fig. 2b). This rise in pH is consistent with the production of OH^- in Eq. 1. Second, the electrokinetic nature of the interparticle attraction was supported by a decrease in its magnitude upon adding salt (Fig. S7), which is known to decrease the magnitude of ionic diffusiophoresis [31-33].

Controlling the phase separation of Ag colloids by adjusting fuel concentrations. It is intuitive to imagine that tuning the concentration of fuel molecules (H_2O_2 in this case) would conveniently control the patterns formed by phase separation, because H_2O_2 concentration is directly related to the reaction rate of eqn. 1. Therefore, increasing H_2O_2 concentration would increase the ionic flux, the magnitude of the resulting electric field, and therefore the strength of the interparticle attraction. However, experiments in Fig. 3b showed the counter-intuitive results that larger clusters were formed at lower H_2O_2 concentrations, while experiments under different H_2O_2 concentrations yielded similar growth kinetics. In addition, clusters formed at higher H_2O_2 concentrations were more branched and less smooth than those found at lower H_2O_2 concentrations.

One possible reason for such discrepancy between experiments and our intuition is that Ag colloids tend to stick to each other at higher ionic strength, which resulted from higher reaction rates at higher H_2O_2 concentrations. In addition, higher H_2O_2 concentrations also leads to stronger inter-particle attraction. As a result, stronger attraction and sticking could prevent particles from freely migrating and prevent clusters from merging, so that more branched, tighter clusters were formed at higher H_2O_2 concentrations. More subtly, the reaction kinetics of Ag could be affected by the H_2O_2 concentration, so that more ions (or ions other than OH^-) could be produced at higher H_2O_2 concentrations [26, 34]. We do not fully understand, nor do we have direct evidence for,

either possibility. However, it is reasonable to argue that adjusting the concentration of H_2O_2 is not an ideal method to control the phase separation of Ag colloids.

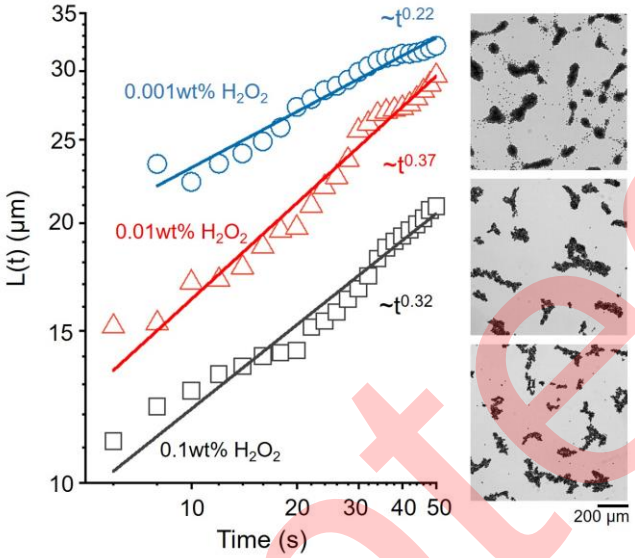

Figure 3 Phase separation of Ag colloids under different H_2O_2 concentrations. From top to bottom: the kinetics and an optical micrograph (t = 50s) of the phase separation of Ag colloids (dark) of φ=17% in 0.001 w.t.%, 0.01 w.t.%, 0.1 w.t.% H_2O_2 aqueous solutions, respectively. Solid lines are linear fits. Both x and y axes are in log10 scales.

Controlling the phase separation of Ag colloids with light: temporal modulation. To more precisely control their phase separation, we introduce an additional repulsive interaction between Ag colloids via photochemistry. This is inspired by earlier studies from the Sen lab [22, 35] and our early studies [36, 37] showing that in the presence of H_2O_2, Cl^- and under UV, Ag colloids spontaneously oscillate between an episode of fast, directional motion and a period of slow, diffusive motion.

In addition to an oscillatory motion, these Ag colloids attract and repel each other when light is turned off and on (Fig. 4a), respectively. As a result, Ag colloids phase separate in the same phenomenological manner as described earlier: individual Ag colloids nucleate into small, interconnected islands that gradually coarsen (Fig. 4c). However, the oscillating population under intermittent illumination phase separated with slower kinetics than non-oscillating Ag colloids without illumination (Fig. 4b). This is likely due to the interparticle repulsion during the half-cycles of UV illumination that impedes the formation of dense clusters. Despite this impedance, clusters still formed because attraction dominated over repulsion over one cycle of light on and off.

The oscillation of Ag colloids in H_2O_2 is speculated to result from oscillatory chemical reactions

occurring on the Ag coating, but details remain elusive and are beyond the scope of this study. Although the chemical details of the oscillation remain unknown, it is reasonable to speculate that the attraction between Ag colloids in the dark is caused by the same oxidation of Ag by H_2O_2 as described in Eqn. 1 and Fig. 2. The repulsion under illumination, on the other hand, is likely to be a reverse reaction, such as the photodecomposition of AgCl, releasing Ag^+ and H^+. To support such speculation, Fig. S8 shows an increase and a decrease in the fluorescence intensity of pH-sensitive fluorescent dyes around such an oscillating Ag colloid when light is switched off and on, respectively, consistent with the production of OH^- and H^+ during these two operations.

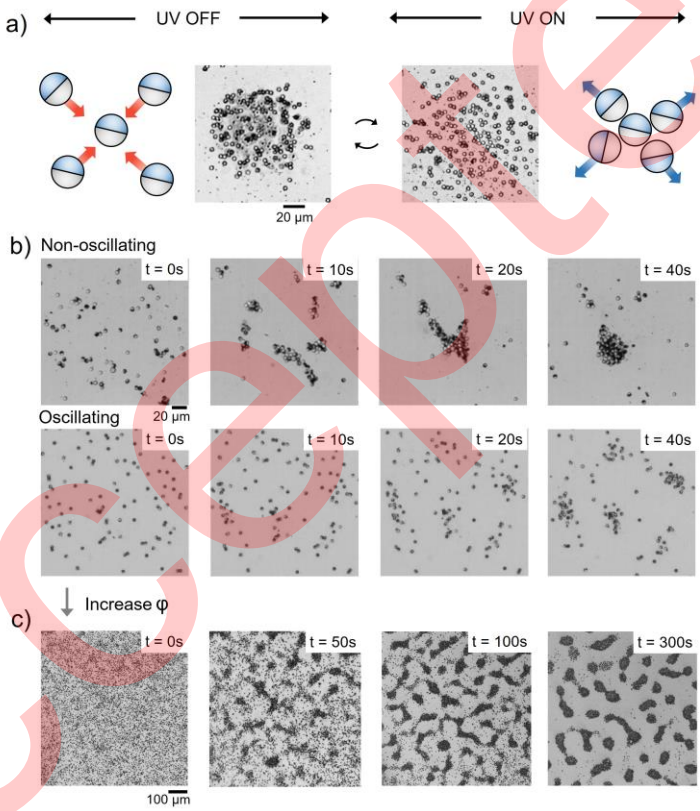

Figure. 4 Phase separation of oscillating Ag colloids under intermittent UV illumination. a) SiO_2-Ag colloids repel each other when light is on, but attract each other when light is off. b) Clustering process of non-oscillating (top) and oscillating (bottom) Ag particles. Top row: Photograph of Ag particles (φ=7.9%) aggregating in 200 μM KCl and 0.25 w.t.% H_2O_2 aqueous solution. Bottom row: In 200 μM KCl and 0.25 w.t.% H_2O_2 aqueous solution, Ag particles (φ=8.1%) aggregated upon switching UV on and off at 0.5 Hz (i.e. 1s light on+1s light off=one cycle). Note that Cl^- is not necessary for the non-oscillating sample to cluster, but was added only to ensure the same solution composition for both samples. c) Optical micrographs of the phase separation of oscillating Ag colloids (φ=17%) at a UV trigger frequency of 0.5 Hz (405 nm, ~126 mW cm^{-2}) at different time instances.

One of the key features of such photoactive oscillating Ag colloids is that the magnitude of their

attraction or repulsion is related to the duration of the light and dark episodes, and thus to the frequency at which light is switched on and off (hereafter referred to as the "trigger frequency"). More specifically, Fig. S9 shows that both attraction and repulsion weaken at higher trigger frequencies, possibly because a high trigger frequency will cause a weak oscillation reaction and thus a weak effective attraction. It is therefore possible to tune the strength of the interparticle interactions by tuning the trigger frequencies. For example, Figure 5a shows that the effective pair-wise attractive force between two Ag colloids, defined as the time-averaged interparticle forces ($\langle F \rangle_t = \frac{\int_0^\tau F(t)dt}{\tau}$), decreased by a factor of three from 0.02 to 0.0073 pN when the trigger frequency was increased from 0.25 to 1 Hz. As a result, both experiments and Brownian dynamics simulations (see SI for details) in Fig. 5b-d and Video S3 show that the phase separation slows down and the characteristic length of the clusters decreases upon increasing the trigger frequency of light. Tuning the trigger frequency of light thus becomes an effective method for tuning both the structure and the growth kinetics of the phase separation patterns of Ag colloids.

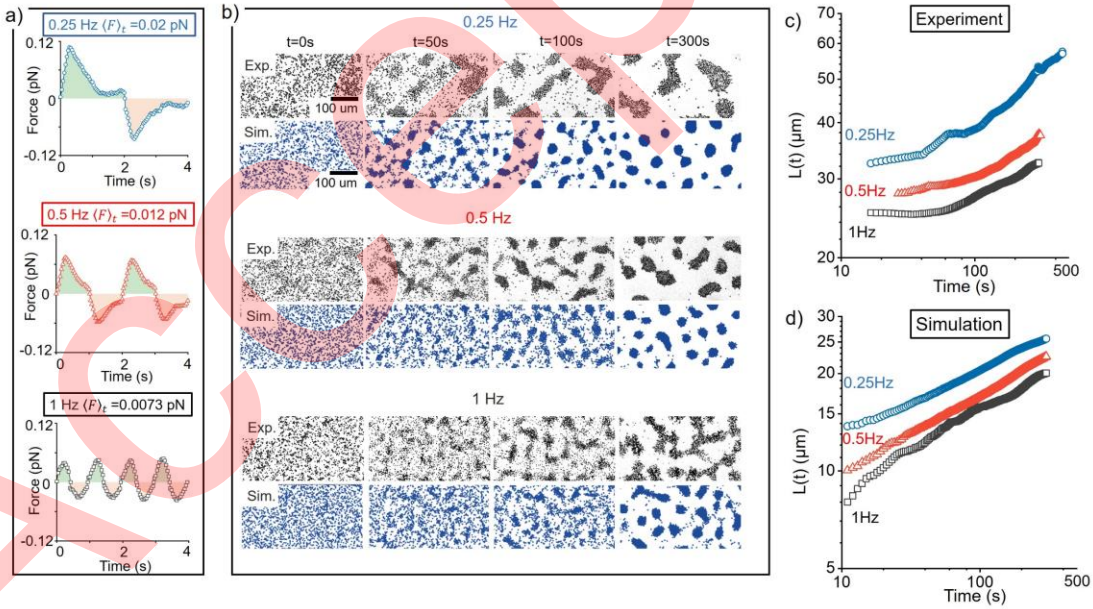

Figure 5 Phase separation at different frequencies of switching light on/off (the "trigger frequency"). a) The change in the interparticle interaction force during one cycle at different trigger frequencies. $<F>_t$ is the time-averaged interparticle forces of the intermittent attraction-repulsion during one cycle. Positive forces are attractive, and the half-cycles of the darkness and illumination are colored in gree and red, respectively. See Supporting Information for measurement of these interparticle forces. b) Optical micrograph (top) and Brownian dynamics simulations (bottom) of the evolution of the phase separation of Ag colloids of φ=17% at different trigger frequencies. c)-d) Characteristic lengths of the patterns in (b). Experiments were carried out in 0.25 w.t.% H_2O_2 and 200 μM KCl aqueous solutions,

using 405 nm light of ~257 mW cm^{-2}. See Supporting Information for simulation details.

Controlling the phase separation of Ag colloids with light: spatial control. In addition to modulating the structure and the kinetics of the phase separation patterns, light can also precisely control *where* the phase separation occurs, as well as dictate the contour of the phase-seperated patterns. Such spatial control takes advantage of structured light technology, which projects arbitrary light patterns of programmable brightness and trigger frequency.

Fig. 6 showcases a number of ways in which the phase separation of Ag colloids was manipulated in space (Video S4). For example, Fig. 6a shows two adjacent regions where Ag colloids formed clusters of different sizes under two light patches of trigger frequencies of 1 and 0.25 Hz, respectively. Fig. 6b and 6c, on the other hand, show that the phase separation of Ag colloids can be limited to regions of different sizes (Fig. 6b) or aspect ratios (Fig. 6c) under corresponding light patterns. In particular, the results in Fig. 6c show that light patches thinner than the characteristic length of a phase-separated Ag cluster forced Ag colloids into bands instead of islands, and the shapes and sizes of these bands followed exactly those of the projected light patterns. This feature was further leveraged to write fine letters with phase-separated Ag colloids (Fig. 6d).

Moreover, the contours of the patterns formed by the phase separation of Ag colloids tended to follow the shapes of the projected light patterns, resulting in patterns with square, circular, hexagonal, or triangular contours (Fig. 6e). This effect is likely due to the fact that only those Ag colloids that are inside a light pattern can be activated. As a result, those that are just inside the light pattern constantly attract particles from outside, increasing the particle concentration at the pattern's edge in the process. These regions then serve as nucleation centers, leading to phase separation patterns that follow the contours of the light patterns.

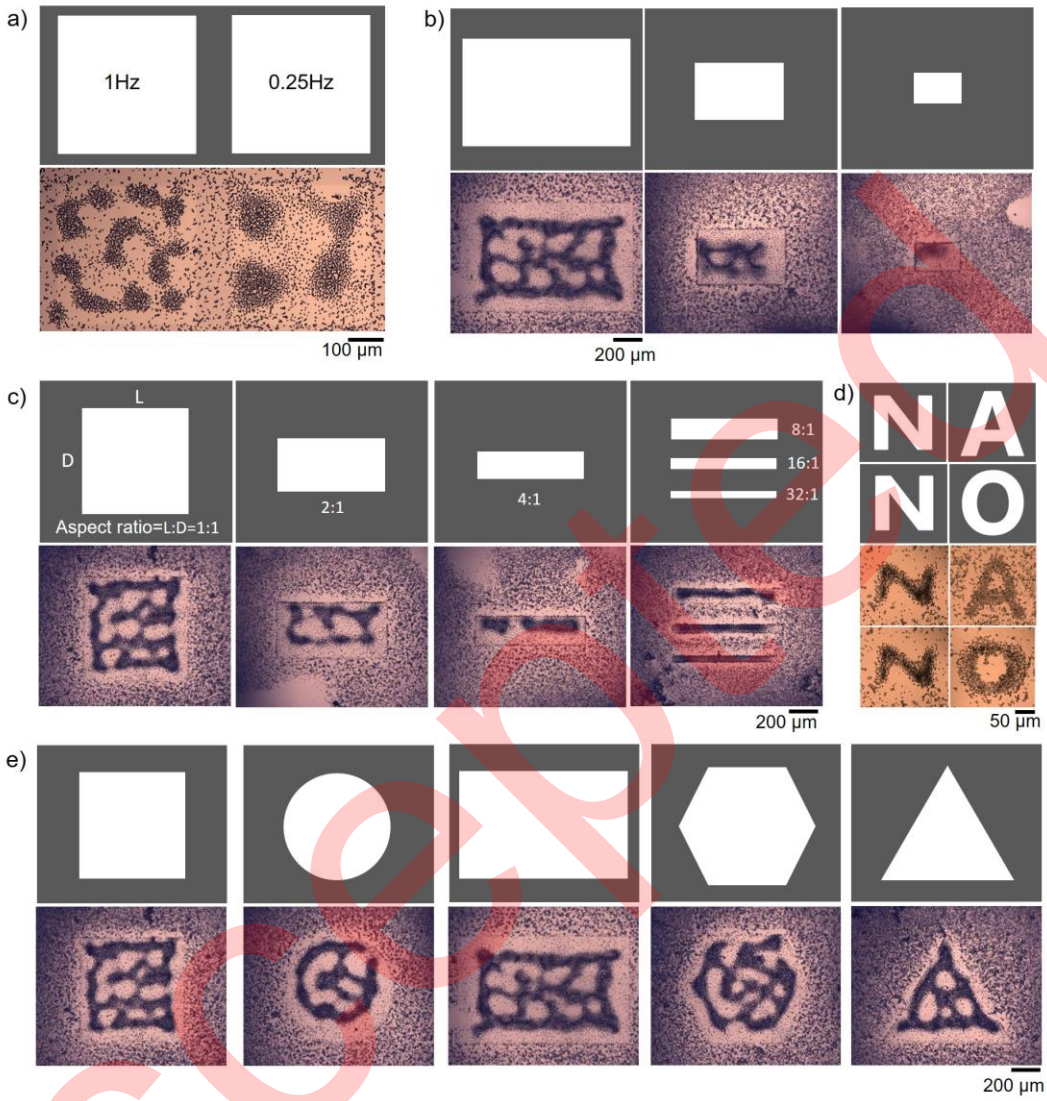

Figure 6 Spatial control of the phase separation of Ag colloids via structured light. a) Two adjacent regions where Ag colloids (φ=14%) formed clusters of different sizes under two light patches of a trigger frequency of 1 (left) and 0.25 Hz (right), respectively. b) Phase separation under light patches of different sizes. c) Phase separation under light patches of different aspect ratios. d) Writing letters of NANO using Ag colloidal clusters with light patches. e) Phase separation under light patches of different shapes. In panel (b-e) the particle density is 28% and the trigger frequency is 1Hz. These experiments were carried out in 0.25 w.t.% H_2O_2 and 200 μM KCl aqueous solutions. The light patches are shown in the top panels of each figure, where the white area is irridated by 405 nm light of ~257 mW cm^{-2}.

DISCUSSION AND CONCLUSION

We have shown that a population of Ag colloids, either Janus SiO_2-Ag microspheres or pure Ag particles, can spontaneously phase separate into dense clusters in H_2O_2. Such phase separation is driven by the attraction of Ag colloids to each other, possibly because Ag oxidizes in H_2O_2 and

generates an electric field that electrophoretically attracts nearby particles. The characteristic length of the formed pattern was quantified and monitored over time, revealing a growth and a coarsening stage with different growth kinetics. Taking advantage of the fact that Ag colloids attract each other in the dark but repel each other under illumination, both the characteristic lengths and the growth kinetics of Ag colloid clusters can be controlled by tuning the trigger frequency of the light, so that higher frequencies lead to smaller clusters that grow more slowly. In addition, light patterns of programmable shapes control where the phase separation occurs, as well as the shape and size of the formed patterns.

The patterns and their growth kinetics were qualitatively reproduced by computer simulations. However, the characteristic length of the clusters formed in the experiment is larger than the corresponding simulation result. Such a difference may be caused by the fact that the interparticle interaction potential in our models is approximated as a constant potential decaying with the interparticle distance, instead of being solved by the reaction-diffusion of chemical species as in the experiments. More specifically, we speculate that the overlap of the concentration fields of many particles within a cluster reduces the attraction of a nearby particle to the cluster, allowing particles outside a cluster to diffuse more freely and clusters to coarsen faster than a simulated cluster without chemical diffusion. The effect of many-body interactions on the phase separation of chemically active colloids is being investigated in a separate study.

On a fundamental level, this study provides insight into the microscopic details of phase separation of chemically active colloids caused by phoretic attraction. Although some qualitative description of the evolutionary kinetics of such a phase separation process has been given in this article, detailed analysis and theory are being sought and will be published separately. On an applied level, this study has used structured light technology to achieve unprecedented spatiotemporal control over the phase separation of chemically active colloids based on the oscillation of Ag colloids under light. Notably, this control has been achieved at the population level, while allowing each individual colloid to move and assemble freely, so that the fine details of the pattern formed are still governed by the intrinsic interplay within the system, rather than dictated by external intervention. Although the colloidal system and its interactions in the current study are entirely chemical in nature, the principle of tuning the effective attraction between individual colloids by alternating between attraction and repulsion can be generally applied to other colloidal systems driven by, for example, electromagnetic fields.

Acknowledgements

We are grateful for the helpful discussions with Profs. Jingyao Tang, Rongpei Shi, and Yongxiang Gao.

Funding

This project is financially supported by the Shenzhen Science and Technology Program (RCYX20210609103122038, JCYJ20210324121408022), and the National Natural Science Foundation of China (T2322006, T2325027, 12274448, 12225410, and 12074243).

Author contributions

Yixin Peng, Wei Wang, Mingcheng Yang, and Hepeng Zhang designed the research. Yixin Peng, Xi Chen, and Chao Zhou performed experiments. Dingyu Xing helped with the measurments of zeta potential. Yixin Peng and Shutong Guo analyzed the data. Longfei Li performed the Brownian dynamics simulations. Wei Wang and Yixin Peng wrote the manuscript. Wei Wang, Mingcheng Yang, and Hepeng Zhang supervised the research.

Conflict of interest

The authors declare no conflict of interest.

Data availability

The original data are available from corresponding authors upon reasonable request.

References

1. Zhang J, Alert R, Yan J *et al.* Active phase separation by turning towards regions of higher density. *Nature Physics*. 2021; **17**(8): 961-967.
2. Zheng J, Chen J, Jin Y *et al.* Photochromism from wavelength-selective colloidal phase segregation. *Nature*. 2023; **617**(7961): 499-506.
3. Zaccarelli E. Colloidal gels: Equilibrium and non-equilibrium routes. *J Phys: Condens Matter*. 2007; **19**(32): 323101.
4. Wang F, Altschuh P, Ratke L *et al.* Progress report on phase separation in polymer solutions. *Adv Mater*. 2019; **31**(26): 1806733.
5. Hooper JB, Schweizer KS. Theory of phase separation in polymer nanocomposites. *Macromolecules*. 2006; **39**(15): 5133-5142.
6. Bialek W, Cavagna A, Giardina I *et al.* Statistical mechanics for natural flocks of birds. *Proceedings of the National Academy of Sciences*. 2012; **109**(13): 4786-4791.
7. van de Koppel J, Gascoigne JC, Theraulaz G *et al.* Experimental evidence for spatial self-organization and its emergent effects in mussel bed ecosystems. *science*. 2008; **322**(5902): 739-742.
8. Linde AD. Phase transitions in gauge theories and cosmology. *Rep Prog Phys*. 1979; **42**(3): 389.
9. Cates ME, Tailleur J. Motility-induced phase separation. *Annu Rev Condens Matter Phys*. 2015; **6**(1): 219-244.
10. Fily Y, Marchetti MC. Athermal phase separation of self-propelled particles with no alignment. *Phys Rev Lett*. 2012; **108**(23): 235702.
11. Buttinoni I, Bialké J, Kümmel F *et al.* Dynamical clustering and phase separation in suspensions of self-propelled colloidal particles. *Phys Rev Lett*. 2013; **110**(23): 238301.
12. Stenhammar J, Tiribocchi A, Allen RJ *et al.* Continuum theory of phase separation kinetics for

active Brownian particles. *Phys Rev Lett*. 2013; **111**(14): 145702.
13. Löwen H. Colloidal dispersions in external fields: recent developments. *J Phys: Condens Matter*. 2008; **20**(40): 404201.
14. Jones MR, Seeman NC, Mirkin CA. Programmable materials and the nature of the DNA bond. *Science*. 2015; **347**(6224): 1260901.
15. Palacci J, Sacanna S, Steinberg AP *et al.* Living crystals of light-activated colloidal surfers. *Science*. 2013; **339**(6122): 936-940.
16. Theurkauff I, Cottin-Bizonne C, Palacci J *et al.* Dynamic clustering in active colloidal suspensions with chemical signaling. *Phys Rev Lett*. 2012; **108**(26): 268303.
17. Ginot F, Theurkauff I, Detcheverry F *et al.* Aggregation-fragmentation and individual dynamics of active clusters. *Nature communications*. 2018; **9**(1): 696.
18. Agudo-Canalejo J, Golestanian R. Active phase separation in mixtures of chemically interacting particles. *Phys Rev Lett*. 2019; **123**(1): 018101.
19. Peng Y, Xu P, Duan S *et al.* Generic rules for distinguishing autophoretic colloidal motors. *Angew Chem Int Ed*. 2022; **61**(12): e202116041.
20. Kagan D, Balasubramanian S, Wang J. Chemically triggered swarming of gold microparticles. *Angew Chem*. 2011; **123**(2): 523-526.
21. Hong Y, Diaz M, Córdova-Figueroa UM *et al.* Light-driven titanium-dioxide-based reversible microfireworks and micromotor/micropump systems. *Adv Funct Mater*. 2010; **20**(10): 1568-1576.
22. Ibele M, Mallouk TE, Sen A. Schooling behavior of light-powered autonomous micromotors in water. *Angew Chem*. 2009; **121**(18): 3358-3362.
23. Trivedi M, Saxena D, Ng WK *et al.* Self-organized lasers from reconfigurable colloidal assemblies. *Nature Physics*. 2022; **18**(8): 939-944.
24. Wu C, Dai J, Li X *et al.* Ion-exchange enabled synthetic swarm. *Nature Nanotechnology*. 2021; **16**(3): 288-295.
25. Gao Y, Wang M, Zhang Z *et al.* Flash Nanoprecipitation Offers Large-Format Full-Color and Dual-Mode Fluorescence Patterns for Codes-in-Code Encryption and Anti-Counterfeiting. *Advanced Photonics Research*. 2022; **3**(11): 2200091.
26. Shah ZH, Wang S, Xian L *et al.* Highly efficient chemically-driven micromotors with controlled snowman-like morphology. *Chem Commun*. 2020; **56**(97): 15301-15304.
27. Chaturvedi N, Hong Y, Sen A *et al.* Magnetic enhancement of phototaxing catalytic motors. *Langmuir*. 2010; **26**(9): 6308-6313.
28. Velegol D, Garg A, Guha R *et al.* Origins of concentration gradients for diffusiophoresis. *Soft matter*. 2016; **12**(21): 4686-4703.
29. Anderson JL. Colloid transport by interfacial forces. *Annual review of fluid mechanics*. 1989; **21**(1): 61-99.
30. Chen X, Xu Y, Zhou C *et al.* Unraveling the physiochemical nature of colloidal motion waves among silver colloids. *Science Advances*. 2022; **8**(21): eabn9130.
31. Brown A, Poon W. Ionic effects in self-propelled Pt-coated Janus swimmers. *Soft matter*. 2014; **10**(22): 4016-4027.
32. Brown AT, Poon WC, Holm C *et al.* Ionic screening and dissociation are crucial for understanding chemical self-propulsion in polar solvents. *Soft Matter*. 2017; **13**(6): 1200-1222.
33. Zhou X, Wang S, Xian L *et al.* Ionic effects in ionic diffusiophoresis in chemically driven active colloids. *Phys Rev Lett*. 2021; **127**(16): 168001.

34. Yan M, Liu T, Li X *et al.* Soft patch interface-oriented superassembly of complex hollow nanoarchitectures for smart dual-responsive nanospacecrafts. *J Am Chem Soc*. 2022; **144**(17): 7778-7789.
35. Ibele ME, Lammert PE, Crespi VH *et al.* Emergent, collective oscillations of self-mobile particles and patterned surfaces under redox conditions. *ACS nano*. 2010; **4**(8): 4845-4851.
36. Chen X, Zhou C, Peng Y *et al.* Temporal Light Modulation of Photochemically Active, Oscillating Micromotors: Dark Pulses, Mode Switching, and Controlled Clustering. *ACS Appl Mater Interfaces*. 2020; **12**(10): 11843-11851. doi: 10.1021/acsami.9b22342
37. Chen X, Zhou C, Peng Y *et al.* Temporal light modulation of photochemically active, oscillating micromotors: Dark pulses, mode switching, and controlled clustering. *ACS applied materials & interfaces*. 2020; **12**(10): 11843-11851.

Supporting Information

Spatio-Temporal Control of the Phase Separation of Chemically Active Immotile Colloids

Yixin Peng[1,#], Longfei Li[2,#], Shutong Guo[3], Xi Chen[1], Chao Zhou[1], Dingyu Xing[4], H. P. Zhang[3,*], Mingcheng Yang[2,*], Wei Wang[1,*]

[1]*School of Materials Science and Engineering, Harbin Institute of Technology (Shenzhen), Shenzhen, Guangdong 518055, China;*

[2]*Beijing National Laboratory for Condensed Matter Physics and Laboratory of Soft Matter Physics, Institute of Physics, Chinese Academy of Sciences, Beijing 100190, China;*

[3]*School of Physics and Astronomy and Institute of Natural Sciences, Shanghai Jiao Tong University, Shanghai, 200240, China;*

[4] *School of Civil and Environmental Engineering, Harbin Institute of Technology (Shenzhen), Shenzhen, Guangdong 518055, China*

#Contributed equally to this work.

*Corresponding authors (emails: weiwangsz@hit.edu.cn (Wei Wang); mcyang@iphy.ac.cn (Mingcheng Yang); hepengzhang@sjtu.edu.cn (H. P. Zhang)

https://engine.scichina.com/doi/10.1360/nso/20230050

Table of Contents

1. Experimental details……..……..

1.1 Preparation of SiO_2-Ag active colloids

SiO_2-Ag microspheres were fabricated by physically depositing a metal layer on top of the SiO_2 microspheres. SiO_2 microspheres of 5 μm in diameter were suspended in ethanol and drop-casted on a piece of pre-cleaned glass slide to prepare a monolayer. The monolayer of SiO_2 was then coated with a 50 nm silver layer via electron beam evaporation (e-beam evaporator, HHV TF500). The as-prepared SiO_2-Ag Janus microparticles were released from the glass slides by ultrasonication and resuspended in deionized water.

1.2 Experimental Setups and particle tracking

The suspension of colloids was observed from underneath with an inverted optical microscope (Olympus IX71). UV light was generated by a LED lamp (Thorlab M365LP1-C1, peak wavelength at 405 nm) and applied from the top. A ring-shaped, white LED lamp is placed around the UV lamp to provide background lighting for imaging, and we confirm that this white light alone cannot activate our micromotors. The motion of the particle was recorded by a CMOS camera (GS3-U3-51S5C-C, Point Grey) typically at 20 frames per second (fps). These videos were then analyzed by MATLAB codes. Particle coordinates were extracted and were used to obtain trajectories and instantaneous speeds of colloids.

A schematic of Structured Light is given in Fig. S1. The core component of this setup is a specialized projector (SM7-405, SICUBE) containing a digital micromirror device (DMD) to project light patterns. It outputs 405 nm light that is capable of exciting SiO_2-Ag colloidal particles. Light patterns are then focused through an objective lens onto the sample stage from below so that some colloids receive purple illumination while others remain in darkness. In addition, a LED lamp (Thorlabs M660L4) that outputs 660 nm light incapable of exciting particles was used to provide background illumination for imaging. A CMOS camera (GS3-U3-51S5C-C, Point Gray) collected images through an objective lens and a tube lens mounted on the other side of the sample stage, with a bandpass filter that removes the 405 nm excitation light but allows for the 660 nm illumination. Videos were recorded typically at 20 frames per second. A computer is connected to the projector to create light patterns of different sizes and shapes generated by Microsoft PowerPoint.

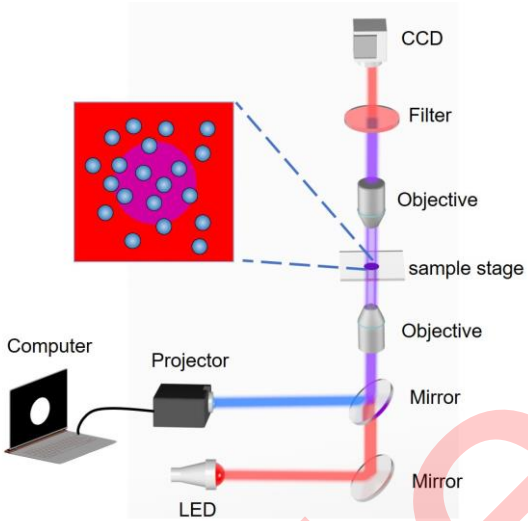

Figure S1 Schematic illustration of the optical setup for generating structured light

1.3 Quantification of population density of colloids

The population density (φ) is determined by the packing fraction of colloids on a 2D plane they reside on, enabled by imageJ recognition. Specifically, we recognized the areas with gray values above 150 in the image and treated their area fraction as the population density. The process is shown in Fig. S2. Note that imageJ calculates the mean grey value of each pixel, therefore the recognized density inevitably deviates from the true value, and the degree of deviation depends on the resolution of the image.

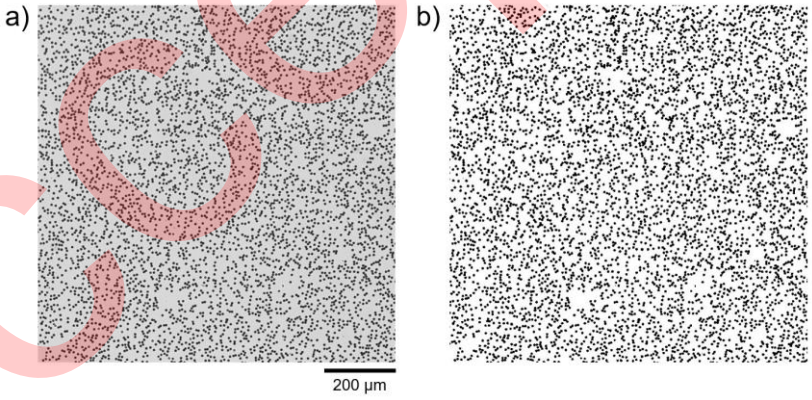

Figure S2 Optical micrographs of SiO_2-Ag at a population density of 17% before (a) and after (b) binary processing by imageJ. The black dots in (b) are SiO_2-Ag and their area percentage is used as population density.

1.4 Definition and quantification of the characteristic length

We calculate the spatial-correlation function G(r) of the image and use the length corresponding to the first root as the characteristic length. The spatial correlation function is written as:

$$\mathrm{G}(\mathbf{r},t)=\sum_{\mathbf{k}} e^{-i\mathbf{k}\cdot\mathbf{r}}S(\mathbf{k},t) \qquad eqn1$$

$$\mathrm{S}(\mathbf{k},\mathrm{t})=\frac{1}{N}\langle|\sum_{j=1}^{N} e^{-i\mathbf{k}\cdot\mathbf{r}_j}(\varphi_j-\bar{\varphi})|^2\rangle \qquad eqn2$$

where **k** is the wave vector, **r** is the radial vector, t is time, S(**k**,t) is the structure-function, and φ is the order parameter representing population density in this study. Then the G(**r**,t) is radially averaged and normalized by G(0,t), and the equation is written as:

$$g(r,t) = \frac{G(r,t)}{G(0,t)} \qquad eqn3$$

Typical g(r) of SiO_2-Ag phase separation at several times is given below. The characteristic length L(t) shown in Figure 1c was obtained from the first root of g(r) (i.e. the smallest r for g(r)=0) at different times.

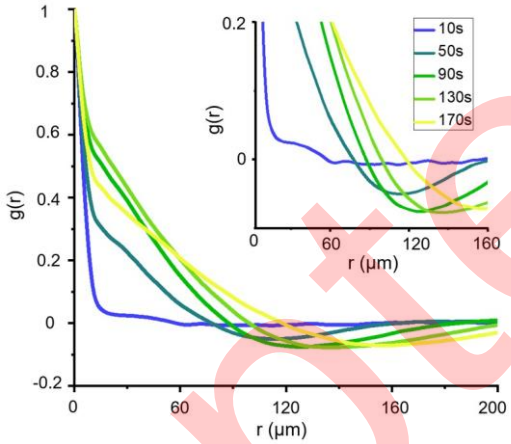

Figure S3. Typical g(r) of SiO_2-Ag phase separation at different time.

2. Brownian dynamics simulation

2.1 Interparticle potential between the oscillating Ag colloid

We tracked all the trajectories of tracers during an on-off light cycle. Fig. S4a shows the trajectories under switching light at 0.25Hz (similar tracking data were also obtained at 0.5 Hz and 1 Hz). The result shows that at the three frequencies the speeds of the tracers when they are attracted or repelled are inversely proportional to the interparticle distance between the central oscillating Ag colloid and tracers (Fig. S4b-c). According to the Stokes equation, both the attractive force and the repulsive force between an oscillating Ag colloid and a tracer sphere scale with 1/r[1], where r is the interparticle distance. The interparticle potential not only decays with distance but also changes with time. Because of the oscillating reaction, both the attractive force and the repulsive force first increase and then decrease with time (Fig. S4d-f). We inferred the autocatalytic reaction is responsible for this[2]. Therefore, the formula of the speed of a tracer is attracted or repelled by an oscillating Ag colloid can be written as a periodic function:

$$\text{Attraction: } u(r,t^*) = \left(\frac{a}{r}\right)\cdot\frac{A^2Bke^{-Akt^*}}{\left(Be^{-Akt^*}+1\right)^2} \quad 0.0 \le t^* < 0.5t_c \qquad eqn4$$

$$\text{Repulsion: } u(r,t^*) = \left(\frac{c}{r}\right)\cdot\frac{A^2Bke^{-Ak(t_c-t^*)}}{\left(Be^{-Ak(t_c-t^*)}+1\right)^2} \quad 0.5t_c \le t^* < t_c \qquad eqn5$$

where t^* is the remainder of time t with a quotient t_c, namely $t = nt_c + t^*(n \in Natural\ number,\ 0 \le t^* < t_c)$. t_c refers to cycle time of the switch light. a, c, A, B, and k are fitting parameters. r is interparticle distance.

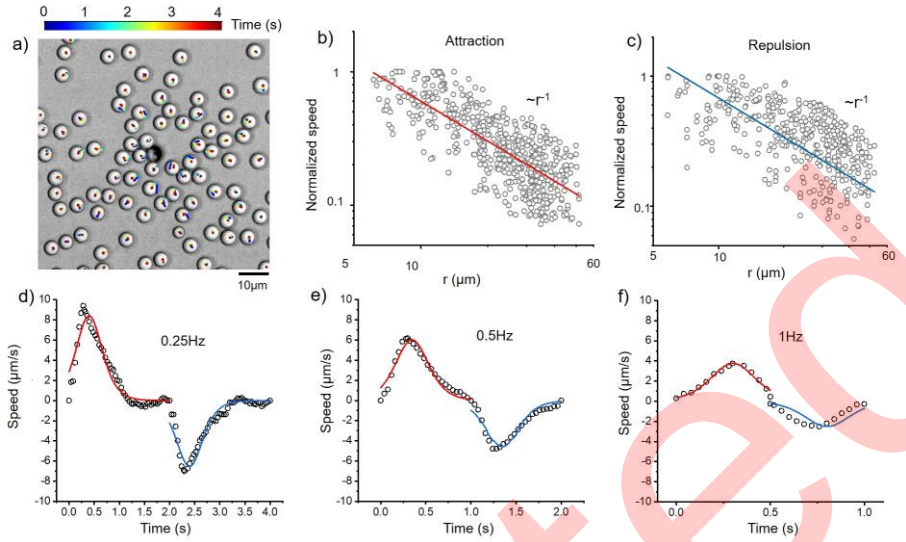

Figure S4. Tracking the motion of the tracers around an oscillating Ag colloid. a) The trajectories of SiO_2 tracers around the central Ag particle for trigger frequency of 0.25 Hz. b) and c) Normalized speeds of tracers when they are attracted (b) or repelled (c). These points represent the speeds of all tracers in 3 consecutive frames at each frequency. These speeds are normalized by the maximum magnitude of speed in each frame. d)-f) During one cycle at a trigger frequency of 0.25 Hz (d), 0.5 Hz (e), or 1 Hz (f), the speeds of the tracers at different times within a circled area 10-15 μm away from the center Ag sphere. A positive value means attraction, and a negative value means repulsion. Black circles are experimental data, and solid lines are fitted by eqn 4 and 5.

2.2 Qualitatively reproduce the phase separation of Ag colloids

We here consider a two-dimensional periodic system composed of $N = 50000$ particles with a diameter σ. The steric interaction between different particles is modeled as a repulsive Lennard-Jones potential, $U(r) = 4[(\sigma/r)^{12} - (\sigma/r)^6] + 1$ if the separation of two particles $r \leq 2^{1/6}\sigma$, $U(r) = 0$ otherwise. In addition, the Ag colloids can attract and repel each other when the light is turned off and on, respectively. This attractive and repulsive force $\boldsymbol{F}_{ij}(\boldsymbol{r}_{ij}, t)$ exerted on particle i by particle j is semi-quantitatively described as a time-dependent pair-wise interaction, yielding $\boldsymbol{F}_{ij}(\boldsymbol{r}_{ij}, t) = -\gamma u(r_{ij}, t)\hat{\boldsymbol{r}}_{ij}$ with an interparticle distance r_{ij} of its unit vector $\hat{\boldsymbol{r}}_{ij}$ and translational friction coefficient γ. The velocity of particle i approaching or moving away from particle j, $u(r_{ij}, t)$, is obtained from experiments and fitted by eqn. 4 and 5 (see section 2.1). Therefore, the motion of particle i is developed by the overdamped Langevin equation

$$\gamma \boldsymbol{v}_i = \boldsymbol{F}_r + \boldsymbol{F}_d + \boldsymbol{\xi} \qquad eqn6$$

where $\boldsymbol{v}_i$ is the particle velocity; $\boldsymbol{F}_r = -\sum_j \partial U(r_{ij})/\partial \boldsymbol{r}_{ij}$ and $\boldsymbol{F}_d = \sum_j \boldsymbol{F}_{ij}(\boldsymbol{r}_{ij}, t)$ refer to the steric interaction force and the attractive (or repulsive) force exerted on particles i by other particles. $\boldsymbol{\xi}$ is the Gaussian-distributed stochastic force with zero mean and variance $\langle \xi_\alpha(t)\xi_\beta(t')\rangle = 2k_B T\gamma\delta_{\alpha\beta}\delta(t-t')$ with α and β Cartesian components and the thermal bath temperature T.

To relate the experiment to simulation system, the one-third of particle diameter, thermal noise $k_B T$ and the total mass of 32000 particles are separately taken as the units of length a_0, energy ε_0 and mass m_0, and the three parameters correspond to $1\,\mu m$, $4.05 \times 10^{-21} J$ (absolute temperature $T = 293K$) and $1\,\mu g$ in the real physical system, respectively. As a result, all other units can be derived from the three quantities. For example, the simulation time unit t_0, $a_0\sqrt{m_0/\varepsilon_0} = 0.5\,s$ and the unit of velocity v_0, $a_0/t_0 = 2\mu m \cdot s^{-1}$. Similarly, the relative velocity $u(r_{ij}, t)$ obtained from the experiment measures, i.e., eqn. 4 and 5 in this supporting information, can be transformed as

$$u(r_{ij},t^*)=\begin{cases}\frac{1}{v_0}\left(\frac{a}{r_{ij}}-\frac{a}{r_{ij}^c}\right)\cdot\frac{A^2Bke^{-Akt_0t^*}}{\left(Be^{-Akt_0t^*}+1\right)^2}, & 0.0\le t_0t^*<0.5t_c\\ \frac{1}{v_0}\left(\frac{c}{r_{ij}}-\frac{c}{r_{ij}^c}\right)\cdot\frac{A^2Bke^{-Ak(t_c-t_0t^*)}}{\left(Be^{-Ak(t_c-t_0t^*)}+1\right)^2}, & 0.5t_c\le t_0t^*<t_c\end{cases} \qquad eqn7$$

Here t_0t^* is the remainder of the time t, similar to the Eqn. 4 and 5, and the terms of $-a/r_{ij}^c$ and $-c/r_{ij}^c$ are introduced to shift $u(r_{ij}^c,t)=0$ at $r_{ij}^c=12\sigma$. Specifically, these fitting parameters at different frequencies of the light switching on/off are listed in Table. S1 as follows:

Table. S1 The fitting parameters in different frequencies.

	a	c	A	B	k
0.25 Hz ($t_c=4$s)	8.3	-6.1	0.63	11.33	9.5
0.5 Hz ($t_c=2$s)	5.0	-4.1	0.47	18.72	17.9
1.0 Hz ($t_c=1$s)	2.4	-1.9	0.31	48.45	41.1

To process, we take $\sigma=3$, $k_BT=1$, $\gamma=14$, and the packing fraction $\rho_0=0.17$ to match the experiment system. In this case, the Peclet number, $P_e=v_0a_0/D$ with $D=k_BT/\gamma$ the translational diffusion coefficient of particle, is consistent between the simulation and experiment system, roughly ensuring the proper mapping of the simulations to those of real physical systems.

3. Supplementary Figures

The phase separation of pure Ag microspheres. In a typical synthesis, 25 mL 0.09 mol/L ascorbic acid aqueous solution was prepared and 1.2698g PVP was added to this solution. Then, 25mL 0.15M $AgNO_3$ was quickly poured into the as-prepared AA solution, the whole process was kept in an ice bath under stirring. Ten minutes later, the above mixture turned from colorless to yellow. The resulting Ag particles (~1 μm) were collected and washed with deionized water and ethanol respectively three times. The Ag particle suspension also showed qualitatively the same phase separation as SiO_2-Ag under 0.001w.t.% H_2O_2 (Fig. S5).

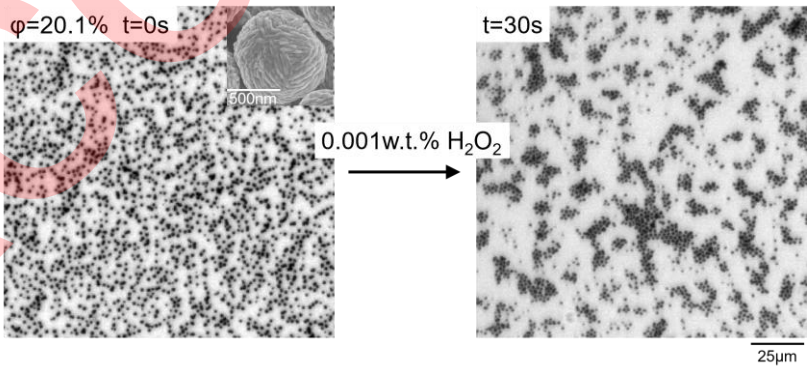

Figure S5. Phase separation of pure Ag particles.

The first derivative of the packing fraction of clusters over time. We calculated the first derivative of the packing fraction of clusters over time in Fig.1d and used the time corresponding to the first root of the derivative to divide the growing and the coarsening (Fig. S6).

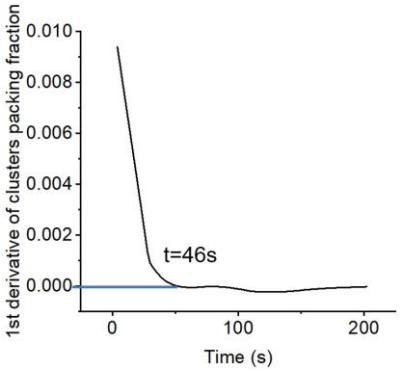

Figure S6. The first derivative of the packing fraction of clusters over time in Fig.1d.

Weakening the attraction of SiO_2-Ag upon the addition of salt. We tracked the trajectories of several SiO_2 tracers when they were attracted by an Ag particle at different salt concentrations. Then their instantaneous speeds were plotted as a function of the interparticle distance between the Ag colloid and SiO_2 tracer. The result (Fig. S7) shows that the attraction of SiO_2-Ag can be weakened by adding salt (KNO_3). This result supports the electrokinetic nature of the interparticle attraction.

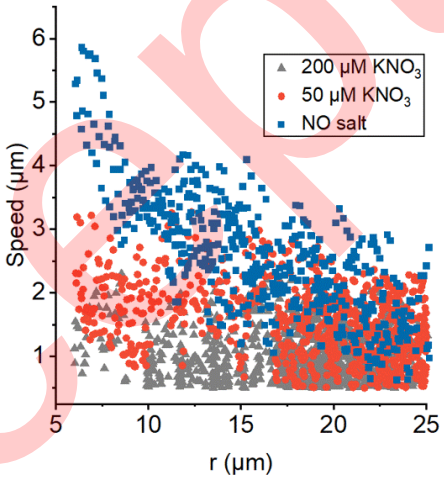

Figure S7 Weakening the attraction of SiO_2-Ag upon the addition of salt in 0.01w.t.% H_2O_2 solution.

Detection of the fluorescence intensity of pH-sensitive fluorescent dyes around an oscillating Ag cluster. The fluorescence intensity increases when the light is turned off and decreases when the light is turned on (Fig. S8).

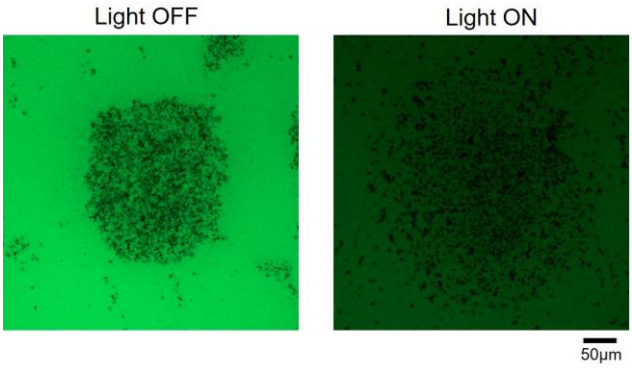

Figure S8. The fluorescence intensity of pH-sensitive fluorescent dyes around a cluster consists of oscillating Ag colloids when the light is switched off and on. Stronger green fluorescence indicates higher pH values. Experiments were carried out in 0.25 w.t.% H_2O_2 and 200 μM KCl aqueous solutions. A pH-sensitive fluorescent dye Solvent Green 7 was used at a concentration of 100 μM.

To avoid the UV quenching fluorescence, the blue light of 475 nm and ~75 mW/cm^2 was used to stimulate the oscillation of Ag particles and excite fluorescence. To observe the fluorescence when the light was off, we turned on the blue light intermittently (0.1s every 2s), we think such a short illumination time hardly affects the oscillation reaction.

Tunable oscillation of an Ag cluster by triggering the frequency of switching light on/off. We use the micro-PIV (Particle Image Velocimetry) to detect the velocity of the Ag particles of a cluster. A video of an oscillating cluster was decomposed into image sequences with a size of 2048 pixel × 2048 pixel by MATLAB, and then the velocity data at each node point (64 × 64 pixel) were extracted as arrows. Fig. S9 shows the peak velocities of particles in a cluster when they are attracted and repelled at different oscillation frequencies. Both attraction and repulsion weaken at higher switching frequencies.

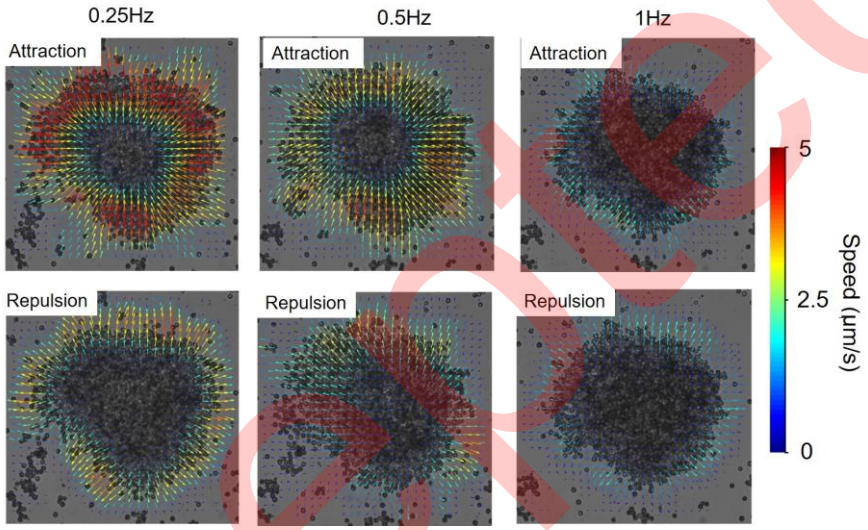

Figure S9. Micro PIV of an Ag cluster oscillated at a trigger frequency of 0.25 Hz, 0.5 Hz, and 1 Hz. Experiments were carried out in 0.25 w.t.% H_2O_2 and 200 μM KCl aqueous solutions, using 405 nm light of ~257 mW/cm^2. The directions of the arrows represent the moving direction of these particles. The colors of the arrows represent the magnitude of the speed.

3. Supplementary Videos

Video S1. The phase separation of 5 μm SiO_2-Ag microspheres in H_2O_2. The population density was 17% and particles were suspended in 0.001w.t.% H_2O_2. These SiO_2-Ag microspheres attract each other in H_2O_2 and form clusters of ~100 μm in size in ~200 s. The Video is played at 15X speed.

Video S2. The phase separation of ~1 μm Ag microspheres in H_2O_2. The population density was 20% and particles were suspended in 0.001w.t.% H_2O_2. These pure Ag microspheres attract each other in H_2O_2 and form clusters of ~20 μm in size in 30 s. The Video is played at 3X speed.

Video S3. The phase separation of oscillating Ag colloid at a trigger frequency of 1 Hz, 0. 5Hz, and 0.25 Hz. The experimental condition: population density is ~17%, 0.25 w.t.% H_2O_2, and 200 μM KCl. An increase in the frequency of switching on/off causes a decrease in the characteristic length of the clusters.

Video S4. Controlling the phase separation of SiO_2-Ag colloids with structured light. The experimental condition: 0.25 w.t.% H_2O_2, 200 μM KCl, and the trigger frequency was 1 Hz. The light patterns of programmable shapes control where the phase separation occurs, and also the shape and size of the patterns formed.

References

1. Möller N, Liebchen B, Palberg T. Shaping the gradients driving phoretic micro-swimmers: influence of swimming speed, budget of carbonic acid and environment. *The European Physical Journal E*. 2021; **44**: 1-17.

2. Steinfeld JI, Francisco JS, Hase WL. *Chemical kinetics and dynamics*. Prentice Hall Upper Saddle River, NJ, 1999.